Chinese Chemical Letters 33 (2022) 3879–3882

Contents lists available at ScienceDirect

Chinese Chemical Letters

journal homepage: www.elsevier.com/locate/cclet

Jigsaw-like mini-pillar platform for multi-mode biosensing

Yongchao Song[b,c], Dongdong Wang[a,b,*], Zehua Li[b], Lirong Wang[b,c], Chuan Fan[b,c], Xuecheng He[b,c], Tailin Xu[b,c,*], Xueji Zhang[b,c]

[a] College of Chemistry and Materials Engineering, Beijing Technology and Business University, Beijing 100048, China
[b] Research Center for Bioengineering and Sensing Technology, University of Science and Technology Beijing, Beijing 100083, China
[c] School of Biomedical Engineering, Health Science Center, Shenzhen University, Shenzhen 518060, China

ARTICLE INFO

Article history:
Received 7 August 2021
Revised 15 October 2021
Accepted 22 December 2021
Available online 27 December 2021

Keywords:
Multiple sensing
Jigsaw-like
Mini-pillar platform
Signal coupling
Microdroplets array

ABSTRACT

The multiple sensing provides booming options to eliminate interference and ensure the accuracy of detection by mutually coupling and validating multiple data sets. Here, we integrate the jigsaw-like multifunctional mini-pillar platform to perform multi-mode (electrochemical, fluorescence, surface-enhanced Raman scattering (SERS) and colorimetric) sensing in individual microdroplets. Each mini-pillar connector can parallelize together by specific concave-convex interface to form integrated jigsaw-like platform for multi-mode sensing, and each specific mini-pillar can be modified into the individual sensing unit to read the prescribed signals. We successfully implemented electrochemical, fluorescence, SERS and colorimetric detection by multiple signals coupling to reduce the false positive analysis. Such platform brings a promising clue of *in-situ* analysis and point-of-care testing for disease diagnosis and health monitoring.

© 2022 Published by Elsevier B.V. on behalf of Chinese Chemical Society and Institute of Materia Medica, Chinese Academy of Medical Sciences.

The sequential operation droplet array has emerged as a powerful tool for medicine, biology, chemistry, physics, and materials science [1–7]. For example, microfluidic-based droplet operations that integrate droplet generation, splitting, fusion, addressing, capture and sorting are famous for cell-related applications [8–11]. Recently, emerging open-channel droplet platform such as superwettable surface, paper-based and mini-pillar microchips with the capabilities of easy solution manipulation also have been advanced in diverse areas such as high-throughput screening, single cell analysis and miniaturized cell experiments [12–18]. By integrating with signal-output approaches such as colorimetric, electrochemical, SERS and fluorescence, the open-channel droplet platform has achieved widespread high-throughput biosensing applications [19–25], providing appreciated blueprint of the *in-situ* analysis and point-of-care testing for disease diagnosis and health monitoring.

Chemical and biological sensors are currently one of the most active areas of analytical research [26–30]. Most advances in sensing technologies and devices are catalyzing key breakthroughs in the detection limit, which have reached the single-molecule level [31–33], while the single-signal output strategy is difficult to provide complete information and unconvincing due to the signal interference from complex sample component and the intrinsic drawbacks of each sensing technology in terms of selectivity and reproducibility. Recently, much efforts have been devoted to coupling the multiple sensing technologies in one chip for parallel detection, and the results are superior to traditional single-signal platforms owing to multiple sets of data coupling and mutual validation [34–39]. For example, the combination of fluorescence and colorimetry on paper-based platform has achieved aptamer-initiated isothermal amplification analysis of glutamate dehydrogenase in clinical samples [36], the coupling of plasmonic circular dichroism and luminescent signals realizes ultrasensitive miRNA *in-situ* quantitation in live cells [40]. These above encouraging results provide unlimited possibilities for accurate, sensitive, rapid and parallel multi-mode sensing in one chip to fulfill the high demands of clinical sensing.

Here, we demonstrate the jigsaw-like mini-pillar platform that confines the analyses in array of open-channel microreactors for electrochemical, fluorescence, SERS and colorimetric multi-mode sensing. Such mini-pillar jigsaw-like platform is established by the programmable 3D printing, modification, splicing and integration. We successfully accomplish electrochemical, fluorescence, SERS and colorimetric multimode sensing on splitable mini-pillar platform, and couple the multi-signal to accurate result output in complex samples. This is the first trial of such jigsaw-like platform to improve the accuracy of detection by multiple signals coupling, which provides an opportunity to develop multi-mode sensing device toward precise physiological and pathological diagnosis.

* Corresponding authors at: Research Center for Bioengineering and Sensing Technology, University of Science and Technology Beijing, Beijing 100083, China.
E-mail addresses: wdd@btbu.edu.cn (D. Wang), xutailin@szu.edu.cn (T. Xu).

https://doi.org/10.1016/j.cclet.2021.12.059
1001-8417/© 2022 Published by Elsevier B.V. on behalf of Chinese Chemical Society and Institute of Materia Medica, Chinese Academy of Medical Sciences.

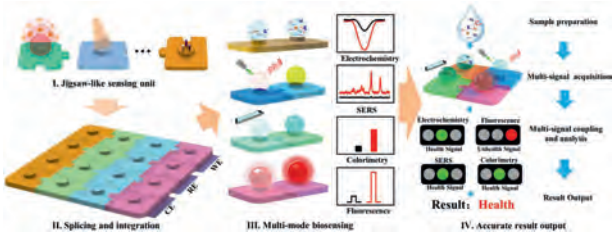

Fig. 1. Schematic of jigsaw-like mini-pillar platform for electrochemical, SERS, colorimetrical, and fluorescence biosensing.

The programmable procedures of jigsaw-like mini-pillar platform including construction and modification, splicing and integration, and multi-mode sensing were illustrated in Fig. 1. In brief, the customized individual mini-pillars with the specific concave-convex interface were first manufactured by 3D printing. Then, in response to different testing requirements, diversified functionalization was applied to mini-pillars. The circuit board stabilized the detachable platform, which is used as a medium for reading batch electrochemical data, and the mini-pillar unit modified by electrodeposition of nanodendritic gold is used to read the SERS signal. Furthermore, with its advantage of droplets anchoring and enrichment, the mini-pillar without other modification could complete the fluorescence and colorimetric detection. The individual and functionalized mini-pillars could realize the array splicing through specific concave-convex interface to form a patterned multi-mode platform for multi-mode sensing. The coupling of multiple results can significantly reduce false positive analysis caused by interference and ambiguous signals, showing huge potentials *in-situ* analysis and point-of-care testing for disease diagnosis and health monitoring.

The jigsaw-like mini-pillar platform exhibits excellent characteristics, which can anchor and enrich trace solutions to achieve multi-mode sensing. The single mini-pillar was manufactured by 3D printing, and the printed polylactic acid (PLA) mini-pillars were successfully assembled into a matrix platform for immobilizing droplets, as shown in Fig. 2a. We further investigated the droplets anchoring ability of the mini-pillar platform in Figs. 2b and c. The droplet (20 μL) was stable on the surface of the inclined and inverted, while Rhodamine 6 G labelled microdroplets on as-prepared platforms presented two diametrically opposed appearances. On the ordinary glass platform, microdroplet was distributed in a relatively large area (Fig. S1a in Supporting information), and there is a clear "coffee ring" after evaporation (Fig. 2d). In contrast, the droplets are uniformly distributed on the surface of the mini-pillar in the designated smaller area (Fig. 2e and Fig. S1b in Supporting information), revealing its excellent enrichment performance. Subsequently, we use 4×4 array as a concept-of-proof to show the splicing and integration process of jigsaw-like mini-pillar platform. The mini-pillars with specific concave-convex interface (Fig. 2f) can be spliced to a complete high-throughput platform for carrying microdroplets.

The functional modification of mini-pillar is the prerequisite for multi-modal sensing. The electrochemical mini-pillar retains the hole array during the 3D printing process, and the embedded electrode array was connected to the circuit board to realize complete electrical signal transmission. The cyclic voltammograms (−0.1∼0.4 V; 10 μL 5 mmol/L hydroxymethyl-ferrocene in PBS buffer) at scan rates from 10 mV/s to 100 mV/s on electrochemical mini-pillar were recorded as shown in Fig. 2g. With the

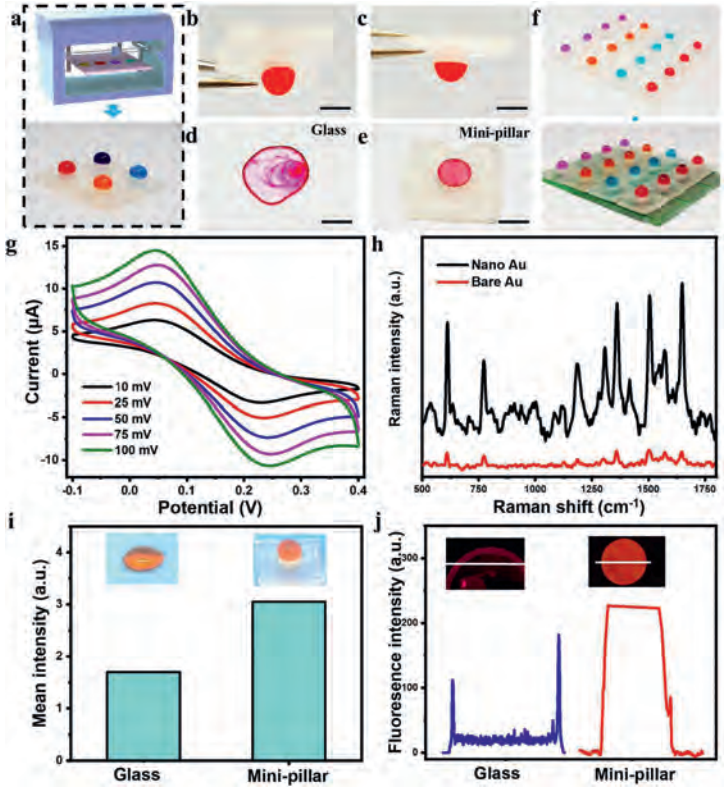

Fig. 2. Characterization of jigsaw-like mini-pillar platform. (a) Individual mini-pillar fabrication by 3D printing. Investigation of the microdroplet adhesion of the mini-pillar platform by (b) sloping and (c) inversing. The enrichment ability of (d) common glass and (e) mini-pillar platform. (f) The splicing and integration process from individual mini-pillar array to jigsaw-like mini-pillar platform. (g) Cyclic voltammetry curves of electrochemical mini-pillar platform at increasing scan rates from 10 mV to 100 mV. (h) The SERS spectra comparison of bare gold mini-pillar platform (red) and nanodendritic gold platform (black). (i) The comparison of colorimetric analysis between common glass and mini-pillar platform. (j) The fluorescence images and corresponding fluorescence intensities of droplets evaporation on glass and mini-pillar. Scale bar: 2 mm.

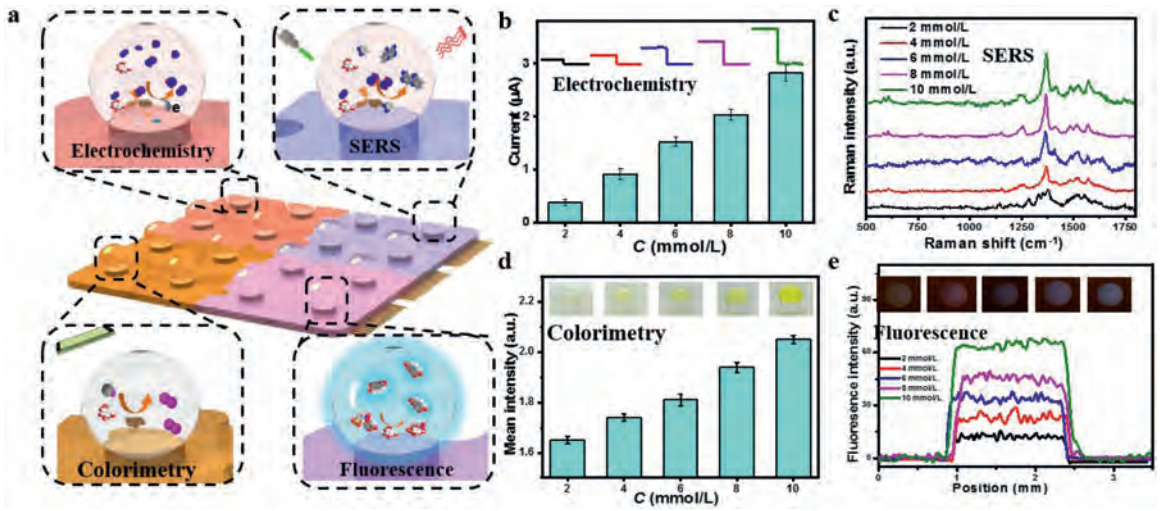

Fig. 3. Jigsaw-like mini-pillar platform toward multi-mode sensing. (a) Schematic illustration of mini-pillar platform for multi-mode glucose detection. (b) Amperometry responses of droplets microarray with glucose concentrations from 2 mmol/L to 10 mmol/L. (c) Raman intensity at 1368 cm^{-1} (2,3-diaminophenazine) of glucose-containing microdroplets from 2 mmol/L to 10 mmol/L. (d) Colorimetrical calibration curve of glucose (2, 4, 6, 8 and 10 mmol/L). (e) The fluorescence images and corresponding intensities of glucose (2, 4, 6, 8 and 10 mmol/L) in microdroplets.

increase of the scan rate, the anode and cathode peak currents increased, and the peak potential remained almost unchanged, indicating that the redox process on the mini-pillars was a surface-limited process. For SERS sensing, first sputter a layer of gold on the micro-pillars to ensure conductivity, as shown in Fig. S2a (Supporting information). Then, the electrolyte composed of HAuCl4 (1 mg/mL) and sulfuric acid (0.5 mol/L) was employed to electrodeposit the nanodendritic gold on the surface of mini-pillar at −1.0 V for 1000 s. In Fig. 2h, we tested the Raman signal enhancement of nanodendritic gold mini-pillar compared with bare gold mini-pillar for possible SERS detection of Rhodamine 6 G (R6G). For the bare gold mini-pillar, all the R6G characteristic peaks were detected with fairly weak signals intensity. In comparison, the Raman intensity on the nanodendrites gold mini-pillar was significantly enhanced as shown in Figs. S2b and c (Supporting information). Benefit from the performance of droplet anchoring and sample enrichment, the mini-pillar can sensitively carry out the fluorescence and colorimetric sensing without additional modification. As displayed in Fig. 2i, the microdroplet (R6G, 10 μL) on mini-pillar presented the more regular and smaller sphere than on common glass and had the obvious enhancement of the gray value. After evaporation, the microdroplets on common glass tended to spread to a larger area and form obvious "coffee ring" spot with stronger fluorescence intensity than the interior of spot, while the distribution of R6G was very homogeneous on mini-pillar with the uniform fluorescence intensity as shown in Fig. 2j. These results indicate that the jigsaw-like mini-pillar platform has excellent performance for electrochemical, SERS, fluorescence and colorimetric multi-mode sensing.

The glucose concentration as the important physiological indicator is tested by electrochemical, SERS and fluorescence and colorimetric multi-mode sensing on such jigsaw-like mini-pillar platform to evaluate its versatility and feasibility (Fig. 3a). In brief, for electrochemical sensing zone, glucose oxidase (1 kU/mL) is modified on the working electrode and then 10 μL glucose (2, 4, 6, 8 and 10 mmol/L) with different concentrations are dropped on electrochemical mini-pillar platform for sensing. The electrochemical detection is performed using chronoamperometry. The glucose is oxidized to gluconic acid and generates hydrogen peroxide, which is then catalyzed at the working electrode under current fluctuations. For SERS sensing zone, 10 μL microdroplet containing glucose oxidase, horseradish peroxidase (HRP) and *o*-phenylenediamine dihydrochloride (OPD) is dropped on mini-pillar, and glucose solution with different concentrations are added for SERS sensing that glucose is catalyzed by glucose oxidase to generate hydrogen peroxide and HRP catalytically oxidized OPD-H_2O_2 with the production of 2,3-diaminophenazine. Then, the Raman spectra of each mini-pillar sites are measured by using a 532 nm laser source with exposure time of 10 s. The colorimetric sensing is performed with the assistance of signal screening by smartphone. The microdroplet containing KI and GOx is dispended on mini-pillar and the colorimetric intensities were increased with the increasing glucose concentration, which are recorded by smartphone and analyzed by using ImageJ analysis software to read the grayscale value. For fluorescence imaging sensing, 3-nitrophenylboronic acid in the droplet can effectively quench the fluorescence of esculetin, and the fluorescence will be restored when glucose is combined with 3-nitrophenylboronic acid.

The results of multi-mode sensing of glucose have simultaneously been recorded by jigsaw-like mini-pillar platform as shown in Figs. 3b–e. In the electrochemical measurements, the electrochemical signal (ΔI) increased gradually with the increase of the glucose concentration, and showed a good linear relationship with a correlation coefficient of 0.9988 (Fig. 3b). For the SERS sensing, specific Raman signals of generated 2,3-diaminophenazine presented at 1368 and 1572 cm^{-1} and increased upon an increase of glucose from 2 mmol/L to 10 mmol/L. It was found that the corresponding calibration chart of the 1368 cm^{-1} peak intensity and the glucose concentration was linear, with a correlation coefficient of 0.9987 (Fig. 3c). In terms of colorimetric verification, color intensities increased with the concentration of glucose with a correlation coefficient of 0.9937 as shown in Fig. 3d. Meanwhile, the fluorescence intensities increased gradually upon an increase of glucose concentration, and showed a good linear relationship, with a correlation coefficient of 0.9743 (Fig. 3e). Thus, we successfully realized electrochemical, SERS, fluorescence and colorimetric multi-mode detection of the glucose on such jigsaw-like mini-pillar platform.

Multi-signal coupling and analysis can effectively avoid the results fluctuation. We further verified ability of such jigsaw-like mini-pillar platform for multi-mode analysis of the specified samples as shown in Fig. 4. Firstly, such platform is employed to detect the glucose concentration in PBS with glucose (6 mmol/L)

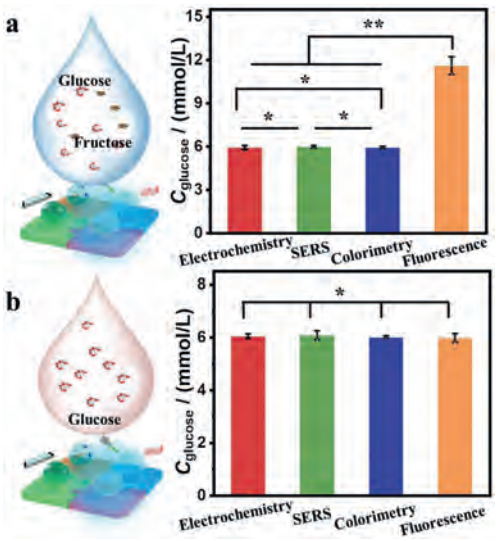

Fig. 4. Jigsaw-like mini-pillar platform toward prescribed sample multi-signal coupling and analysis. (a) Multi-signal integration of glucose and fructose samples in PBS. (b) The electrochemical, SERS, colorimetric and fluorescent results of glucose in diluted serum. $^{*}P > 0.05$, $^{**}P < 0.001$, Student's T-test.

and fructose (6 mmol/L), the results indicate that the concentration of glucose by electrochemical, SERS and colorimetric are similar (5.90 ± 0.14, 5.96 ± 0.09 and 5.91 ± 0.08 mmol/L; $P > 0.05$) while the fluorescent signal has large fluctuations due to the weak selectivity of the fluorescence method for sugars (11.59 ± 0.62 mmol/L; $P < 0.001$) (Fig. 4a). Thus, by multi-signal coupling, error signals of fluorescence can be removed, the final glucose concentration was finally calculated as 5.92 ± 0.11 mmol/L. Then, we further employ such platform to detect the glucose (6 mmol/L) in diluted human serum (containing various proteins, 1:10 diluted with 0.1 mol/L PBS, pH 7.0). The results of four signals have no obvious difference (6.05 ± 0.08, 6.08 ± 0.17, 6.01 ± 0.06 and 5.98 ± 0.17 mmol/L; $P > 0.05$) indicate that each method can realize the accurate detection of glucose in serum sample without obvious interference (Fig. 4b). Such multi-mode results of the same analyses greatly reduce the false positive analysis due to the intrinsic drawbacks of the signal sensing technology by multiple data coupling, difference analyzing and results confirmation, which brings a promising clue of *in-situ* analysis and point-of-care testing for disease diagnosis and health monitoring.

In conclusion, we have demonstrated a jigsaw-like mini-pillar platform for electrochemical, fluorescence, SERS and colorimetric multi-mode sensing. Each mini-pillar as individual sensing unit can read out the relevant signal from microdroplets and parallelize mini-pillars splice by specific concave-convex interface to form an integrated multi-signal transmission platform for multi-mode sensing. Multifunctional modifications allow such jigsaw-like mini-pillar platform to achieve the multiple and quantitative detection. The excellent abilities of mini-pillar for anchoring and enriching the trace solution provide an ideal platform for fluorescence and colorimetric sensing, and the embedded electrode array can achieve electrochemical analysis, and electrodeposited nanodendritic gold substrate can realize SERS sensing. We employed such jigsaw-like platform to detection of trace glucose in PBS and diluted serum by multiple signals coupling, the results indicate that the integrated platform can discharge the interference and ensure the accuracy of detection by multiple signals coupling. Such jigsaw-like mini-pillar platform can easily perform high-throughput detection with the advantages of high-yield, low sample volume, multiple signal options, no cross contamination and simple to disassemble and splice, demonstrating the potential application of *in-situ* analysis and point-of-care testing for disease diagnosis and health monitoring.

Declaration of competing interest

The authors declare no competing interests.

Acknowledgments

We acknowledge funding from National Natural Science Foundation of China (Nos. 21804007 and 21890742), Youth Scholars of Beijing Technology and Business University (No. QNJJ2020–04), and SZU Top Ranking Project (No. 86000000210), Shenzhen Stability Support Plan (No. 20200806163622001).

Supplementary materials

Supplementary material associated with this article can be found, in the online version, at doi:10.1016/j.cclet.2021.12.059.

References

[1] G. Villar, A.J. Heron, H. Bayley, Nat. Nanotechnol. 6 (2011) 803–808.
[2] T. Xu, L.P. Xu, X. Zhang, S. Wang, Chem. Soc. Rev. 48 (2019) 3153–3165.
[3] A.O. Delawder, J.C. Barnes, Nat. Chem. 12 (2020) 328–330.
[4] Q. Sun, D. Wang, Y. Li, et al., Nat. Mater. 18 (2019) 936–941.
[5] B. Zheng, J.D. Tice, R.F. Ismagilov, Adv. Mater. 16 (2004) 1365–1368.
[6] L. Sun, F. Bian, Y. Wang, et al., Proc. Natl. Acad. Sci. U. S. A. 117 (2020) 4527–4532.
[7] Y. Song, T. Xu, X. Song, X. Zhang, Adv. Funct. Mater. 30 (2020) 1910329.
[8] D. Mark, S. Haeberle, G. Roth, F. von Stetten, R. Zengerle, Chem. Soc. Rev. 39 (2010) 1153–1182.
[9] R.H. Cole, S.Y. Tang, C.A. Siltanen, et al., Proc. Natl. Acad. Sci. U. S. A. 114 (2017) 8728–8733.
[10] L. Shang, Y. Cheng, Y. Zhao, Chem. Rev. 117 (2017) 7964–8040.
[11] Z. Zhu, C.J. Yang, Acc. Chem. Res. 50 (2017) 22–31.
[12] H. Li, Q. Yang, G. Li, et al., ACS Appl. Mater. Interfaces 7 (2015) 9060–9065.
[13] M. Benz, M.R. Molla, A. Boser, A. Rosenfeld, P.A. Levkin, Nat. Commun. 10 (2019) 2879.
[14] C. Parolo, A. Merkoci, Chem. Soc. Rev. 42 (2013) 450–457.
[15] M.M. Gong, D. Sinton, Chem. Rev. 117 (2017) 8447–8480.
[16] J.L. Garcia-Cordero, Z.H. Fan, Lab Chip 17 (2017) 2150–2166.
[17] D. Tian, Y. Song, L. Jiang, Chem. Soc. Rev. 42 (2013) 5184–5209.
[18] W. Feng, E. Ueda, P.A. Levkin, Adv. Mater. 30 (2018) 1706111.
[19] X. He, T. Xu, W. Gao, et al., Anal. Chem. 90 (2018) 14105–14110.
[20] H. Liu, Z. Yang, L. Meng, et al., J. Am. Chem. Soc. 136 (2014) 5332–5341.
[21] Y. Song, T. Xu, J. Xiu, X. Zhang, Biosens. Bioelectron. 149 (2020) 111845.
[22] H. Zhang, T. Oellers, W. Feng, et al., Anal. Chem. 89 (2017) 5832–5839.
[23] T.M. Yen, T. Zhang, P.W. Chen, et al., ACS Nano 9 (2015) 10655–10663.
[24] H. Li, Q. Yang, J. Hou, et al., Adv. Funct. Mater. 28 (2018) 1800448.
[25] X. Song, T. Xu, Y. Song, et al., Talanta 218 (2020) 121206.
[26] Y. Liu, X. Dong, P. Chen, Chem. Soc. Rev. 41 (2012) 2283–2307.
[27] M.E. Roberts, S.C. Mannsfeld, N. Queralto, et al., Proc. Natl. Acad. Sci. U. S. A. 105 (2008) 12134–12139.
[28] V. Schroeder, S. Savagatrup, M. He, S. Lin, T.M. Swager, Chem. Rev. 119 (2019) 599–663.
[29] T. Xu, W. Shi, J. Huang, et al., ACS Nano 11 (2017) 621–626.
[30] J. Wang, Chem. Rev. 108 (2008) 814–825.
[31] G.G. Gregorio, M. Masureel, D. Hilger, D.S. Terry, et al., Nature 547 (2017) 68–73.
[32] J. Jarvius, J. Melin, J. Goransson, et al., Nat. Methods 3 (2006) 725–727.
[33] B.A. Flusberg, D.R. Webster, J.H. Lee, et al., Nat. Methods 7 (2010) 461–465.
[34] J.A. Adkins, K. Boehle, C. Friend, et al., Anal. Chem. 89 (2017) 3613–3621.
[35] Z. Guo, Y. Jia, X. Song, et al., Anal. Chem. 90 (2018) 6124–6130.
[36] C.Y. Hui, M. Liu, Y. Li, J.D. Brennan, Angew. Chem. Int. Ed. 57 (2018) 4549–4553.
[37] J.C. Harper, T.L. Edwards, T. Savage, et al., Small 8 (2012) 2743–2751.
[38] W. Duan, X. Wang, H. Wang, F. Li, Talanta 180 (2018) 76–80.
[39] Y. Song, T. Xu, L.P. Xu, X. Zhang, Chem. Commun. 55 (2019) 1742–1745.
[40] S. Li, L. Xu, W. Ma, et al., J. Am. Chem. Soc. 138 (2016) 306–312.